

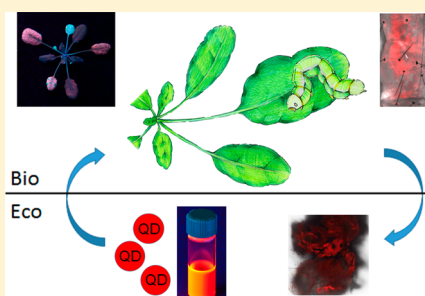
Fluorescence Reports Intact Quantum Dot Uptake into Roots and Translocation to Leaves of *Arabidopsis thaliana* and Subsequent Ingestion by Insect Herbivores

Yeonjong Koo,^{*,†} Jing Wang,[‡] Qingbo Zhang,[§] Huiguang Zhu,[§] E. Wassim Chehab,[†] Vicki L. Colvin,[§] Pedro J. J. Alvarez,[‡] and Janet Braam^{*,†}

[†]Department of BioSciences, [‡]Department of Civil & Environmental Engineering, and [§]Department of Chemistry, Rice University, Houston, Texas 77005, United States

S Supporting Information

ABSTRACT: We explored the impact of quantum dot (QD) coat characteristics on NP stability, uptake, and translocation in *Arabidopsis thaliana*, and subsequent transfer to primary consumers, *Trichoplusia ni* (*T. ni*). *Arabidopsis* was exposed to CdSe/CdZnS QDs with three different coatings: Poly(acrylic acid-ethylene glycol) (PAA-EG), polyethylenimine (PEI) and poly(maleic anhydride-*alt*-1-octadecene)-poly(ethylene glycol) (PMAO-PEG), which are anionic, cationic, and relatively neutral, respectively. PAA-EG-coated QDs were relatively stable and taken up from a hydroponic medium through both *Arabidopsis* leaf petioles and roots, without apparent aggregation, and showed generally uniform distribution in leaves. In contrast, PEI- and PMAO-PEG-coated QDs displayed destabilization in the hydroponic medium, and generated particulate fluorescence plant tissues, suggesting aggregation. PAA-EG QDs moved faster than PEI QDs through leaf petioles; however, 8-fold more cadmium accumulated in PEI QD-treated leaves than in those exposed to PAA-EG QDs, possibly due to PEI QD dissolution and direct metal uptake. *T. ni* caterpillars that fed on *Arabidopsis* exposed to QDs had reduced performance, and QD fluorescence was detected in both *T. ni* bodies and frass, demonstrating trophic transfer of intact QDs from plants to insects. Overall, this paper demonstrates that QD coat properties influence plant nanoparticle uptake and translocation and can impact transfer to herbivores.



INTRODUCTION

Possible uptake and accumulation of nanoparticles (NPs) in plants, especially in the edible parts, has raised great concern over human exposure from food web contamination.¹ However, very few studies have investigated the possibility of NP transfer from plant uptake into a potential food web, with those published focused on aquatic^{2–5} and microbial^{6,7} systems. For example, poly(acrylic acid)-octylamine-coated CdSe/ZnS was found to be transferred from zooplankton to zebrafish (*Danio rerio*) with a biomagnification factor (BMF) of 0.04.³ Over 5-fold biomagnification of uncoated CdSe quantum dots (QDs) was also observed in protozoa (*Tetrahymena thermophila*) when QDs were transferred from bacteria (*Pseudomonas aeruginosa*).⁷ Transfer of carboxylated and biotinylated QDs from ciliated protozoan to rotifers was also reported.⁶ Nevertheless, studies on NP transfer in a terrestrial ecosystem, from primary producers (e.g., plants) to primary consumers (e.g., pests), are very limited,^{8,9} with one report showing transfer of Au NPs of different sizes from tobacco (*Nicotiana tabacum* L. cv *Xanathi*) to tobacco hornworm (*Manduca sexta*) with 6.2, 11.6, and 9.6 BMF for 5, 10, and 15 nm Au NPs, respectively.⁸ However, there remains a critical knowledge gap in trophic transfer of NPs in food chains more closely relevant to human consumption.

Furthermore, the mechanism(s) underlying NP uptake and translocation by plants remains poorly understood. NP solutions are dynamic, being able to aggregate and dissolve. In addition, plants can take up various ions from the growth medium or soil and reductively precipitate them as particles.^{10–13} Therefore, the presence of particles in a plant is not always definitive proof for the plant's ability to take up and translocate intact metal NPs. QDs are particularly suited for studying intact NP uptake in plants. In addition to being useful for tracking particle uptake and movement in a variety of organisms,^{14–17} fluorescence is only detected when intact QDs are present. Furthermore, breakdown components are very unlikely to reconstitute into fluorescent QDs in plants, especially within the original narrow light spectrum.^{18,19} Another issue to consider in NP uptake and translocation by plants is the effect of NP surface coatings. Many types of metallic NPs, including the core ions of QDs, are coated by a polymer surface to increase stability, water-solubility, and usefulness (e.g., enhancement of biocompatibility for bioimaging applications).^{14,15,20–23} Once released into the environ-

Received: October 17, 2014

Revised: November 27, 2014

Accepted: December 1, 2014

Published: December 1, 2014

ment, the coatings could affect NP interactions with plants. The effect of such NP surface coatings has been explored in a limited number of studies.^{10,15,22} It was previously demonstrated that QDs with NH₂ groups composing the surface coat were able to translocate to plant aerial tissues,²⁴ and QDs conjugated with two different polymers also showed different uptake rates by poplar.²⁵ Zhai et al. reported the transport of Au NPs through poplar plasmodesmata,²⁶ although it is unknown whether this transport pattern also applies to other NPs, such as QDs, and whether NP surface coats affect their translocation pattern throughout the whole plant.^{27,28}

In this report, we report on the effect of QD coats on particle stability and plant uptake and translocation, and trophic transfer to a generalist herbivore. We chose QDs for this study because, as nanoscale fluorescent semiconductors, they enable tracking of intact particle uptake and movement. In addition, we chose to use *Arabidopsis thaliana*, a member of Brassicaceae family; therefore the findings may be relevant to diverse and popular vegetables, such as cabbage, kale, and broccoli. Furthermore, the extensive tools and resources available for this model plant will facilitate future investigations of the underlying molecular genetic and genomic bases for differential NP uptake, translocation, and toxicity.

MATERIALS AND METHODS

QD Synthesis and Characterization. QDs were synthesized as described in Zhu et al.³² For surface modification of QDs, the as-synthesized QD core was transferred to aqueous solution using ligand exchange or encapsulation methods.^{29,30} PAA-EG³⁰ and PMAO-PEG³¹ were synthesized using procedures described previously³² and PEI (MW = 25000) (408727, Sigma-Aldrich, St. Louis, MO) was purchased from Sigma-Aldrich. A 0.1 mL aliquot of polymer solution was added to 1 mL of ethyl ether solution of QDs under stirring; 1 mL of water was then added to the solution and sonicated for 2 min. The mixture was stirred overnight to evaporate ethyl ether. The nanoparticles were purified by ultracentrifugation at 183 000g and 0.2 μm syringe filtration. Purified nanoparticles were redispersed in deionized water. Uniform cores and core sizes were characterized with TEM imaging.²⁵ QD concentrations were determined by chemical digestion with ICP-MS (Elan 9000, PerkinElmer, MA), as described below. The zeta potential of each QD solutions was determined with Zen 3600 Zetasizer Nano (Malvern Instruments, United Kingdom) at 10 μg/mL concentration. Differential stability of QD fluorescence, indicating particle structural integrity and QD tendency to aggregate in plant growth media and water are reported in the Supporting Information (Figure S1).

Plant Growth and QD Treatments. QDs were dispersed in water or 1/4, 1/8, or 1/16-strength of Hoagland solution³³ at 10 μg/mL Cd concentration. *Arabidopsis* were grown in soil or hydroponically in Hoagland solution, as described in the text, under cycles of 12-h light (100 μmol/m² s)/12-h dark at 23 °C, 75% relative humidity. For detached leaf petiole assays, 4-week-old soil-grown *Arabidopsis* plants were used as sources of leaves. Leaf petioles were cut 1 mm from the main stem and the cut edge was placed immediately into a drop of media with or without QDs, as indicated, on a glass slide up to 1-h (Supporting Information, Figure S2A). The detached leaves were placed under 25 μmol/m² s of light to maintain transpiration. For whole plant hydroponics, seed holder components of Araponic hydroponic culture system (Kit 140 HD, Araponics, Belgium) were used. *Arabidopsis* seeds were

sown on 0.8% agar, with 1/16 strength of Hoagland solution, within the seed holder. After germination, single *Arabidopsis* plants were grown in 15 mL conical tubes for 4 weeks and then transferred to 1/16-strength Hoagland solution containing either PAA-EG or PEI QDs at 10 μg/mL for 7 days before analysis.

Confocal Microscopy and Fluorescence Measurement. A confocal microscope, LSM 710 (Zeiss, Germany) equipped with 514 nm laser for excitation, was set at 580 to 620 nm for harvesting spectra for QD detection and avoiding endogenous fluorescence of plant tissues. The laser strength was set at 3000 and gain values were set at 900 in the operating software Zeiss ZEN 2010 (Zeiss, Germany). QD fluorescence strengths were measured with Infinte 200 pro (Tecan, Switzerland) plate reader at 514 nm excitation and 600 nm emission.

Whole plant photographs were taken with a Nikon D80 digital camera using UV365 nm light exposure with a UVGL-58 (UVP, Upland, CA) hand-held UV lamp.

ICP-MS Analysis. Quantitative cadmium (Cd) and selenium (Se) analyses were done following the method described previously.³⁴ QD-treated *Arabidopsis* were harvested and frozen in liquid nitrogen immediately. Harvested samples were ground using TissueLyser II (Qiagen, Germantown, MD) and dried completely at 100 °C for 48 h before determining dry weight. After overnight digestion with 70% HNO₃ (A509, Fisher Scientific, PA) and 30% of H₂O₂ (H325, Fisher Scientific, PA) samples were filtered with 0.2 μm of syringe filters (28145, VWR International, Radnor, PA). Cd and Se elements were analyzed with Elan 9000 apparatus ICP-MS (PerkinElmer, Waltham, MA). The plant extraction method was verified by comparing the Cd and Se recovery from direct solubilization of QDs to Cd and Se to plant leaves injected with QDs; no significant differences in recovery were found between the samples. Germanium was used for the internal standard for recovery and injection control. A standard curve was obtained from 1, 2, 4, 8, 16, and 32 ng/mL of Ge, Cd, and Se ion injection, and the regression coefficient was over 0.99.

Trichoplusia ni Treatment. For cabbage looper *Trichoplusia ni* (*T. ni*) treatment, *Arabidopsis* were grown in 1/4-strength Hoagland solution for 4 weeks and 16 *Arabidopsis* plants were transferred to media containing QDs in 1/16-strength Hoagland solution. Plants were grown for 3 days in the presence of 10 μg/mL of QDs, at which point no signs of toxicity were apparent, before *T. ni* treatment. *T. ni* handling was performed as previously described.^{35,36} Eggs of the *T. ni* were purchased from Benzon Research, Inc. (Carlisle, PA). Fifteen newly hatched *T. ni* larvae were transferred with a fine brush onto the 16 *Arabidopsis* plants for each treatment group. *Arabidopsis* and *T. ni* samples were harvested 7 days after *T. ni* transfer. Harvested *T. ni* were analyzed with both confocal microscopy and ICP-MS, and the remaining *Arabidopsis* leaves were also analyzed with ICP-MS. *Arabidopsis* growth and *T. ni* treatment were carried out at 23 °C, 50% relative humidity under 24-h continuous light at 25 μmol/m² s light intensity.

Statistical Analyses. Standard deviations are indicated as error bars for all data sets. Statistical significances between data were calculated by the student *t* test with two-tailed distribution. Data with *p* values below 0.05 or 0.01 are indicated as significantly different.

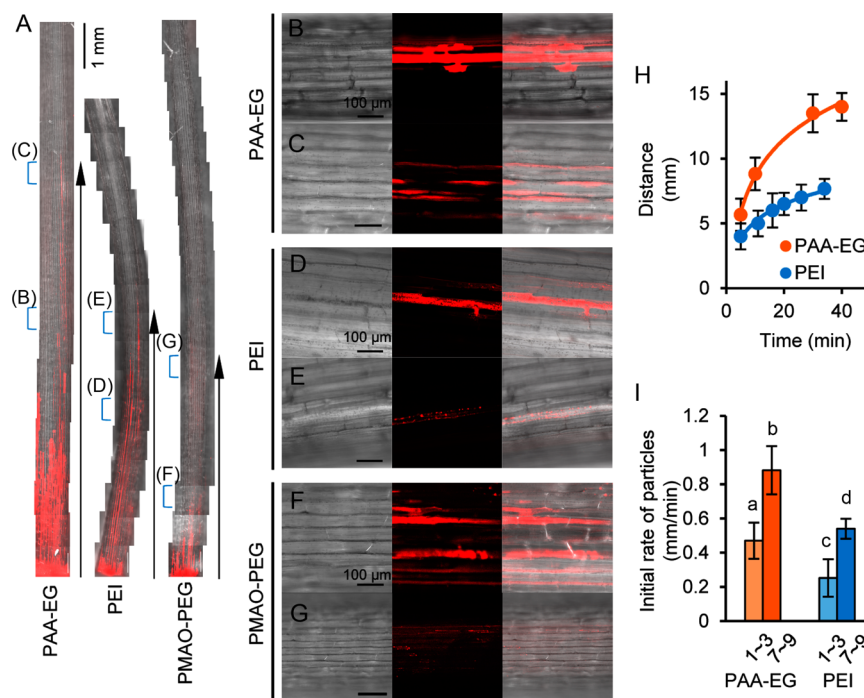


Figure 1. QD uptake into detached *Arabidopsis* leaves. (A) Confocal fluorescence localization in leaf petioles after a 1-h exposure to PAA-EG, PEI, and PMAO-PEG QDs. Cut petiole edge is at bottom. Arrows designate regions of fluorescence detection, with arrowhead indicating the most distal fluorescence signal. The 7th to 9th leaves of 4-week-old *Arabidopsis* were used for analysis. (B–G) Higher resolution images at midrange sites (B, D, and F) and at end points (C, E, and G) of fluorescence detection as labeled in panel A. Left column shows confocal fluorescence, and right column is overlay of left and middle panels. (H) Translocation distances of PAA-EG and PEI QDs over time in the main vein of the 9th leaves of 4-week-old plants; $n = 3$. (I) Translocation rates dependent on QD coat and leaf age. Distance from the petiole cut sites of fluorescence detected within 10 min of QD exposure. The x-axis indicates leaf number of older leaves (leaves 1–3) or younger leaves (leaves 7–9); $n \geq 4$.

RESULTS AND DISCUSSION

QD Coat Characteristics Affect Particle Uptake Rate and Translocation through *Arabidopsis* Leaf Petioles. To first assess QD translocation through *Arabidopsis* leaf tissue in the absence of complications or restrictions that could arise from root uptake, we examined movement of QD through freshly cut leaf petioles. Petioles were immersed into 1/16-strength Hoagland solution containing 10 $\mu\text{g}/\text{mL}$ of QDs with PAA-EG, PEI, or PMAO-PEG coats (Supporting Information, Figure S2A). All three types of QDs were readily visible at the cut petiole base under confocal analysis within 1 h of leaf exposure to the QDs (Figure 1A). However, only the PAA-EG and PEI QDs were detectable as multiple elongated fluorescence traces beyond 15 mm from the cut petiole base (Figure 1A–G), suggesting efficient translocation. The QDs appeared to travel through contiguous cells, likely major vascular tissues, but with some leakage occurring to neighboring cells (Figure 1B–F and Supporting Information, Figure S2B). The smooth appearance of the PAA-EG QD-treated plant cells suggests that the negatively charged coat may enable relatively fluidic movement through the plant vascular tissue (Figure 1, Figure S2B). Fluorescence became less uniform as the translocation distance from the cut site increased (Figure 1A–G). PAA-EG QD fluorescence at distal sites was strongest along the edges of plant cells (Figure 1C), as if adhering against cell membranes or walls. Whereas the *in planta* PAA-EG QD fluorescence appeared smooth and uniform, the PEI and PMAO-PEG QD fluorescence had a particulate appearance (Figure 1, Figure S2B), suggesting particle aggregation. Only minimal fluorescence could be

detected in distal petiole regions from PMAO-PEG QD-exposed leaves despite strong fluorescence at the petiole base. The strong PMAO-PEG QDs fluorescence at the petiole base and minimal fluorescence detected more distally are findings consistent with the interpretation of *in vitro* behavior that the PMAO-PEG QD particles may readily aggregate (Figure S1). Therefore, PMAO-PEG QDs may form particles of sizes and/or structures that are incapable of efficient translocation through plant tissues. These data demonstrate that once introduced directly into the vascular tissue of *Arabidopsis* leaf petioles, PAA-EG and PEI QD particles can move through the petiole, whereas PMAO-PEG particles fail to translocate readily, possibly because of PMAO-PEG QDs aggregation tendencies. These findings are consistent with previous work that showed that nanomaterial coats can influence plant uptake and translocation.^{21,23,25,37}

To assess the role of *Arabidopsis* leaf age in QD movement, we compared translocation rates of PAA-EG and PEI QDs in younger leaves to that in older leaves. Petioles of younger rosette leaves, that is, the seventh, eighth, and ninth leaves to form during rosette development, transported both PAA-EG and PEI QDs faster on average than the petioles of rosette leaves that developed first, second, and third (Figure 11; a and b, $p < 0.01$; c and d, $p < 0.01$). PAA-EG QDs traveled through the petioles of younger leaves at an average rate of 0.9 mm/min and through older leaf petioles at an average rate of 0.5 mm/min, whereas PEI QDs moved at a rate of about half that of PAA-EG QDs in both the younger and older rosette leaves (b and d, $p < 0.01$; a and c, $p < 0.05$) (Figure 11). The increased translocation within younger *Arabidopsis* leaf petioles may be

the consequence of enhanced transpiration related to more rapid leaf growth and expansion and/or robust photosynthesis.

Uptake of QDs by *Arabidopsis* Roots and Translocation in Planta. To address whether intact plants can take up and translocate QDs, we next assessed whether QDs presented to *Arabidopsis* roots can be found in distinct plant organs. We did not include the PMAO–PEG QDs in this analysis because of their aggregation behaviors (Supporting Information, Figures S1 and S3) and reduced movement and lack of continuous fluorescence through leaf vascular tissue (Figure 1).

Inductively coupled-mass spectroscopy (ICP–MS) detection of significant Cd and Se levels in leaves of QD-treated *Arabidopsis* relative to levels found untreated control plants (Figure 2A; “PAA-EG” and “PEI” versus “NT”) is consistent with uptake of either intact particles or of breakdown components of the QDs. Indeed, on the basis of our QD translocation results (Figure 1), we would have expected more Cd and Se to be found in the leaves of *Arabidopsis* exposed to PAA-EG QDs than in the leaves of plants exposed to the PEI QDs. Our data, however, indicate that *Arabidopsis* treated with the PEI QDs accumulated approximately 8-fold more Cd and 2.5-fold more Se in their leaves than the PAA-EG QD-treated plants. Similar results of preferential accumulation of Cd and Se in shoot tissues of poplar plants exposed to PEI QDs than in shoot tissues of poplar exposed to PAA-EG QD were reported previously.²⁵ We interpret these results to indicate that at least a substantial portion of the Cd and Se detected in the leaves of QD-treated *Arabidopsis* is from uptake of Cd and Se directly and not because of intact QD presence. Consistent with this interpretation is our finding that the leaves of *Arabidopsis* treated with QDs coated with either PAA-EG or PEI accumulated more Se than Cd (Figure 2A), with Cd/Se ratios of 0.16 and 0.47, respectively. Intact QDs have more Cd in their cores than Se; the Cd/Se ratio of PAA-EG QDs is 2.19 and the ratio for PEI QDs is 1.97. The lower Cd/Se ratio detected in the *Arabidopsis* leaves is consistent with the effective absorption of Se ion or related organic compounds into plants.^{25,38} The different Cd/Se ratios observed for the two different QDs suggest that there is differential interaction of the ions with the coat components that may influence availability for *Arabidopsis* root uptake and/or translocation through the plant tissues.

As shown in Figure 2B, *Arabidopsis* plants whose roots were exposed to QDs for 7 days showed signs of leaf stress. Leaves of PAA-EG QD-treated plants showed increased chlorosis, with a lighter green leaf coloration compared to the untreated control (Figure 2B). Leaves of plants exposed to PEI QDs also lost green coloration and appeared brown and smaller than leaves of untreated plants (Figure 2B). The higher toxicity of PEI QDs than PAA-EG QDs is consistent with the findings that PEI QDs lost fluorescence and therefore likely dissolved after dilution (Supporting Information, Figure S1) and that plants treated with PEI QDs accumulated much more Cd and Se than plants exposed to the more stable PAA-EG QDs (Figure 2A, Figure S1).

To more directly detect uptake and translocation of intact QDs, we monitored QD fluorescence, which would be present only if the QD core remained intact. Bright fluorescence emissions were easily detected in the rosette leaves of QD-treated *Arabidopsis*. Plants that were exposed to PAA-EG QDs emitted clear fluorescence of varying intensity from nearly all leaves (Figure 2C) and the leaves that fluoresced showed

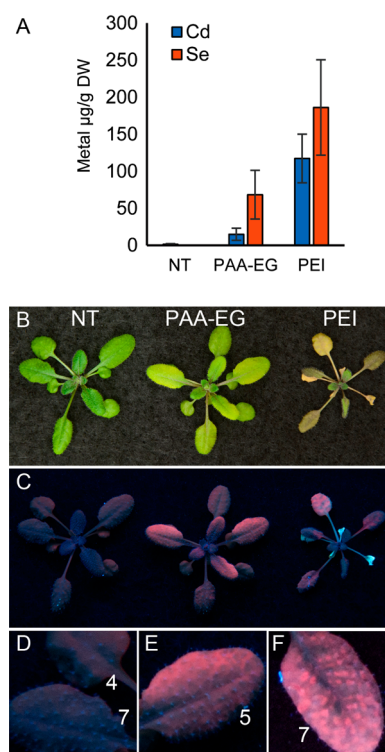


Figure 2. Rosette leaf Cd and Se accumulation levels, overall appearance, and fluorescence detection after root exposure to 10 µg/mL QDs. Four-week-old *Arabidopsis* plants were transferred to 1/16 strength Hoagland solution with QDs and grown for 7 days. (A) Leaf levels of Cd and Se, the core elements of QDs, were quantified by ICP–MS. $n \geq 4$. (B) Representative photographic images of shoots after 7 days of incubation with QDs. (C) Fluorescence detection under UV_{365 nm} of shoots shown in panel B. (D–F) Higher magnification of individual leaves in panel C. “NT”, not treated with QDs.

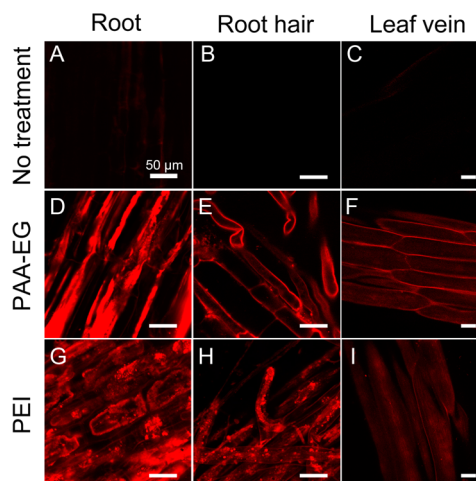


Figure 3. Confocal analysis of QD localization pattern in *Arabidopsis* roots, root hairs, and leaf veins. Root, root hairs, and leaf veins of nontreated plants (A–C) and plants whose roots were exposed to either PAA-EG QDs (D–F) or PEI QDs (G–I). All images were collected under similar exposure conditions. Size bars = 50 µm.

relatively uniform fluorescence distribution over the entire leaf (Figure 2E), thus providing evidence for uptake and translocation of the PAA-EG QDs from the roots to the aerial leaves. Although when detached, younger leaves showed greater translocation rates than older leaves (Figure 11); whole plants

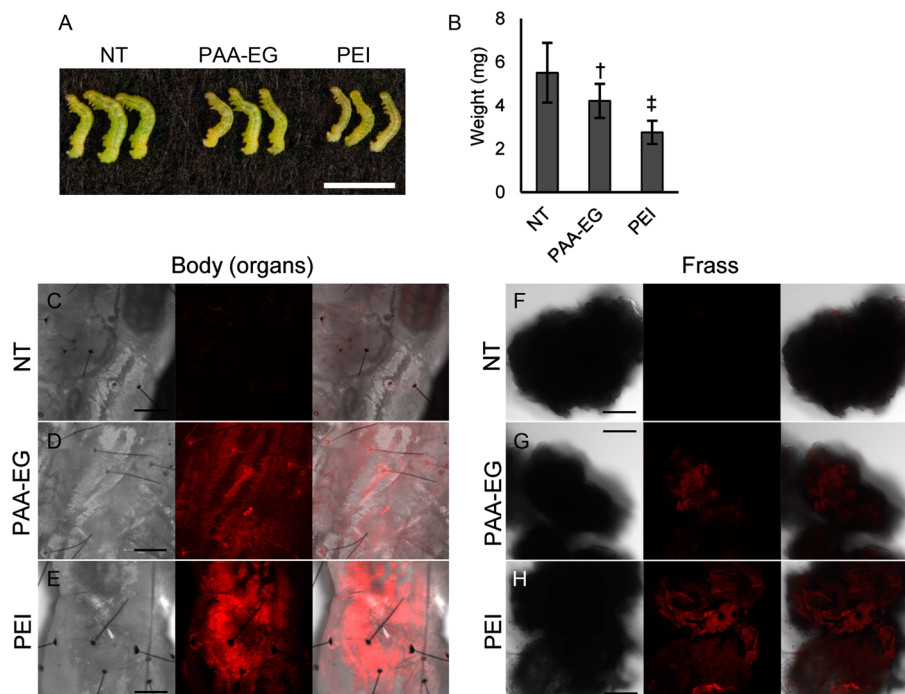


Figure 4. Performance of and fluorescence in *T. ni* caterpillars fed on QD-treated *Arabidopsis*. Newly hatched *T. ni* caterpillars were placed on 4-week-old *Arabidopsis* that were exposed to no QDs (NT), PAA-EG QDs, or PEI QDs. (A,B) Caterpillar weight was measured after 7 days of feeding. Bar = 5 mm. $n \geq 10$. † indicates $p < 0.05$, and ‡ indicates $p < 0.01$ difference from NT; t -Test. (C–E) Bright-field (left column), confocal fluorescence (middle column), and superimposed bright-field and confocal (514 nm excitation/580–620 nm emission, red) (right column) images of *T. ni*. (F–H) Frass produced by *T. ni* analyzed as in panels C–E. Size bars = 200 μ m.

whose roots were exposed to PAA-EG QDs showed more fluorescence in a subset of midaged leaves. This pattern may reflect that the leaves undergoing greatest growth and expansion during the one-week treatment period may be most likely to accumulate PAA-EG QDs. Comparative analysis of individual leaves shows that the fifth leaf to develop had higher fluorescence than older leaves (leaves 2–4), which were more fully developed when the QD exposure began.

PEI QDs exposed plants also showed leaf fluorescence but overall levels may be lower than that of leaves of PAA-EG QD-treated plants, possibly because of toxicity-induced leaf damage (Figure 2C). Higher resolution analysis of individual leaves showed that PEI QD fluorescence was not uniform but instead appeared as distinct spots on the leaves (Supporting Information, Figure S4). In older leaves of PEI QD-treated plants, the fluorescence appeared as broad patches around the major veins, but in younger leaves the fluorescence was either present as distinct large puncta (Figure S4, leaves 3 and 4) or was very low (Figure S4, leaf 5). Such uneven distribution, as also seen in detached leaf petioles (Figure 1D,E), suggests that the PEI QDs may have aggregated once in the plant tissues. These data demonstrate that *Arabidopsis* can readily take up QDs from aqueous solution and transport them as intact particles through plant tissues. This work is consistent with other findings of NP uptake by plants.^{39–42} Our use of distinct coatings and low salt plant growth media may be the basis for our successful detection of QD uptake compared to a previous report indicating a lack of QD uptake and translocation by *Arabidopsis*.¹⁸

Confocal microscopic images demonstrate that both PAA-EG and PEI QDs accumulated within cells of the main root, root hairs, and leaf veins; however, the patterns of fluorescence were distinct (Figure 3). The PAA-EG QD fluorescence

appeared as long traces along root cells and as outlines of root hairs and leaf vein cells (Figure 3D–F), consistent with possible apoplastic localization. Fluorescence from the PEI QDs showed particulate patterns in the root tissues and intracellular fluorescence in the leaf vein cells (Figure 3G to I). The fluorescence patterns of the PEI QDs suggest that the particles aggregated in root cells but that those that reached the leaf vein may have flowed freely within the intracellular spaces.

***Trichoplusia ni* Caterpillars Accumulate QDs after Feeding on QD-Exposed *Arabidopsis*.** To test whether NP uptake and accumulation may make the translocated particles available for herbivore ingestion, we presented *Arabidopsis* that had been exposed to QDs for 3 days to newly hatched *T. ni* caterpillars larvae and allowed the herbivore to feed for 7 days. The *T. ni* caterpillars were weighed after the feeding period to assess herbivore performance. *T. ni* that fed on *Arabidopsis* plants exposed to either the PAA-EG QDs or PEI QDs weighed only 80% ($p < 0.05$, $n \geq 10$) and 50% ($p < 0.01$, $n \geq 10$), respectively, of the weight of *T. ni* caterpillars that fed on control plants, which were not exposed to QDs (Figure 4A,B). The reduced weight gain of *T. ni* that fed on the QD-treated plants could be due to toxicity of the plant-derived QDs and/or Cd or Se released from the QD cores. Alternatively, the QD-treated plant material may have been less palatable or nutritious to the herbivore. Overall plant damage observed after caterpillar feeding is consistent with the conclusion that plant exposure to either PAA-EG or PEI QDs reduced caterpillar feeding; untreated plants had fewer rosette leaves remaining after the 7 days feeding period (Supporting Information, Figure S5A).

Compared to the low level of background fluorescence detected in *T. ni* that fed on control plants not exposed to QDs (Figure 4C), higher fluorescence was readily detected within the *T. ni* caterpillars that fed on QD-treated plants (Figure

4D,E). Similarly, whereas the frass of caterpillars that fed on control plants had only background fluorescence (Figure 4F), the frass from the caterpillars that fed on the QD-treated plants had elevated fluorescence (Figure 4G,H). The caterpillars that fed on plants treated with PEI QDs appeared to have higher fluorescence than those that fed on plants treated with PAA-EG QDs (Figure 4D,E,G,H). The fluorescence strength in the caterpillar frass and the overall frass appearance were similar regardless of the QD coat used in the plant treatment.

The *T. ni* caterpillars and frass also have detectable levels of Cd and Se, with higher levels in the insects that fed on plants exposed to PEI QDs than PAA-EG QDs (Supporting Information, Figure S5B). However, much of the trace metal content found in the insects and frass is likely not associated with intact QDs, but instead derived from ions released from unstable QDs and accumulated in plant tissues. Finding less Cd and Se in frass from the insects that fed on PEI QD-treated plants than those that fed on PAA-EG QD-treated plants is consistent with possible greater retention of PEI QDs in the insect body. To assess the efficiency of transfer and biomagnification, we compared the quantities of trace metal accumulation in the plants, insects, and insect frass and calculated trophic transfer factors (TTF). The TTFs for trace metals for PAA-EG QD-treated *Arabidopsis* to *T. ni* and from *T. ni* to frass were close to 1, whereas the transfer factor of PEI QD-treated *Arabidopsis* to *T. ni* was also close to 1, the TTF for *T. ni* to frass was 0.28. The poor transfer of PEI QD-derived trace metals from *T. ni* to frass may reflect accumulation in *T. ni*.

In summary, use of QD fluorescent detection provides strong evidence for *Arabidopsis* uptake of intact nanoparticles. The coat of the particle greatly influences particle stability, aggregation properties, and plant toxicity. In addition, both the particle coat and leaf age affect particle uptake rate and translocation. Understanding the role of the nanoparticle coats for plant interaction is important for informed manipulation of plant properties by nanoparticle introduction.^{21,43,44} Furthermore, because terrestrial plants are a foundational component of the ecosystem, the impact of nanoparticle uptake on plants themselves and on the herbivores that rely on plants for nutrition are important environmental and ecological concerns.

■ ASSOCIATED CONTENT

■ Supporting Information

Data and description for QD stability in solution, three-dimensional QD fluorescence images in leaf petioles, magnified fluorescence images of leaves under UV light, and metal quantities in *T. ni* and their frass after feeding on *Arabidopsis* leaves. This material is available free of charge via the Internet at <http://pubs.acs.org>.

■ AUTHOR INFORMATION

■ Corresponding Authors

* (J.B.) Phone: (713) 348-4277; e-mail: braam@rice.edu.

* (Y.K.) Phone: (713) 348-6963; e-mail: yeonjong@rice.edu.

■ Notes

The authors declare no competing financial interest.

■ ACKNOWLEDGMENTS

This material is based upon work supported by the National Science Foundation under Grant No. CMMI 1057906. The authors thank Joann Pan for experimental support, A. Budi

Utama for assistance with confocal microscopy, and Jin Young Koo for her TOC art work.

■ REFERENCES

- (1) Rico, C. M.; Majumdar, S.; Duarte-Gardea, M.; Peralta-Videa, J. R.; Gardea-Torresdey, J. L. Interaction of nanoparticles with edible plants and their possible implications in the food chain. *J. Agric. Food Chem.* **2011**, *59* (8), 3485–98.
- (2) Bouldin, J. L.; Ingle, T. M.; Sengupta, A.; Alexander, R.; Hannigan, R. E.; Buchanan, R. A. Aqueous toxicity and food chain transfer of quantum dots in freshwater algae and *Ceriodaphnia dubia*. *Environ. Toxicol. Chem.* **2008**, *27* (9), 1958–1963.
- (3) Lewinski, N. A.; Zhu, H.; Ouyang, C. R.; Conner, G. P.; Wagner, D. S.; Colvin, V. L.; Drezek, R. A. Trophic transfer of amphiphilic polymer coated CdSe/ZnS quantum dots to *Danio rerio*. *Nanoscale* **2011**, *3* (8), 3080–3083.
- (4) Lee, W.-M.; An, Y.-J. Evidence of three-level trophic transfer of quantum dots in an aquatic food chain by using bioimaging. *Nanotoxicology* **2014**, *0*, 1–6.
- (5) Zhu, X.; Wang, J.; Zhang, X.; Chang, Y.; Chen, Y. Trophic transfer of TiO₂ nanoparticles from daphnia to zebrafish in a simplified freshwater food chain. *Chemosphere* **2010**, *79* (9), 928–933.
- (6) Holbrook, R. D.; Murphy, K. E.; Morrow, J. B.; Cole, K. D. Trophic transfer of nanoparticles in a simplified invertebrate food web. *Nat. Nanotechnol.* **2008**, *3* (6), 352–355.
- (7) Werlin, R.; Priester, J. H.; Mielke, R. E.; Krämer, S.; Jackson, S.; Stoimenov, P. K.; Stucky, G. D.; Cherr, G. N.; Orias, E.; Holden, P. A. Biomagnification of cadmium selenide quantum dots in a simple experimental microbial food chain. *Nat. Nanotechnol.* **2011**, *6* (1), 65–71.
- (8) Judy, J. D.; Unrine, J. M.; Bertsch, P. M. Evidence for biomagnification of gold nanoparticles within a terrestrial food chain. *Environ. Sci. Technol.* **2010**, *45* (2), 776–781.
- (9) Judy, J. D.; Unrine, J. M.; Rao, W.; Bertsch, P. M. Bioaccumulation of gold nanomaterials by *Manduca sexta* through dietary uptake of surface contaminated plant tissue. *Environ. Sci. Technol.* **2012**, *46* (22), 12672–12678.
- (10) Beattie, I. R.; Haverkamp, R. G. Silver and gold nanoparticles in plants: Sites for the reduction to metal. *Metallomics* **2011**, *3* (6), 628–32.
- (11) Petersen, E. J.; Henry, T. B.; Zhao, J.; MacCusprie, R. I.; Kirschling, T. L.; Dobrovolskaia, M. A.; Hackley, V.; Xing, B.; White, J. C. Identification and avoidance of potential artifacts and misinterpretations in nanomaterial ecotoxicity measurements. *Environ. Sci. Technol.* **2014**, *48* (8), 4226–46.
- (12) Gardea-Torresdey, J. L.; Parsons, J. G.; Gomez, E.; Peralta-Videa, J.; Troiani, H. E.; Santiago, P.; Yacaman, M. J. Formation and growth of Au nanoparticles inside live alfalfa plants. *Nano Lett.* **2002**, *2* (4), 397–401.
- (13) Gardea-Torresdey, J. L.; Gomez, E.; Peralta-Videa, J. R.; Parsons, J. G.; Troiani, H.; Jose-Yacaman, M. Alfalfa sprouts: A natural source for the synthesis of silver nanoparticles. *Langmuir* **2003**, *19* (4), 1357–1361.
- (14) Yu, W. W.; Chang, E.; Drezek, R.; Colvin, V. L. Water-soluble quantum dots for biomedical applications. *Biochem. Biophys. Res. Commun.* **2006**, *348* (3), 781–6.
- (15) Medintz, I. L.; Uyeda, H. T.; Goldman, E. R.; Mattoussi, H. Quantum dot bioconjugates for imaging, labelling and sensing. *Nat. Mater.* **2005**, *4* (6), 435–46.
- (16) Ballou, B.; Lagerholm, B. C.; Ernst, L. A.; Bruchez, M. P.; Waggoner, A. S. Noninvasive imaging of quantum dots in mice. *Bioconjugate Chem.* **2004**, *15* (1), 79–86.
- (17) Lewinski, N. A.; Zhu, H.; Jo, H. J.; Pham, D.; Kamath, R. R.; Ouyang, C. R.; Vulpe, C. D.; Colvin, V. L.; Drezek, R. A. Quantification of water solubilized CdSe/ZnS quantum dots in *Daphnia magna*. *Environ. Sci. Technol.* **2010**, *44* (5), 1841–6.
- (18) Navarro, D. A.; Bisson, M. A.; Aga, D. S. Investigating uptake of water-dispersible CdSe/ZnS quantum dot nanoparticles by *Arabidopsis thaliana* plants. *J. Hazard Mater.* **2012**, *211–212*, 427–35.

- (19) Mancini, M. C.; Kairdolf, B. A.; Smith, A. M.; Nie, S. Oxidative quenching and degradation of polymer-encapsulated quantum dots: New insights into the long-term fate and toxicity of nanocrystals in vivo. *J. Am. Chem. Soc.* **2008**, *130* (33), 10836–7.
- (20) Dietz, K. J.; Herth, S. Plant nanotoxicology. *Trends Plant Sci.* **2011**, *16* (11), 582–9.
- (21) Zhu, Z. J.; Wang, H.; Yan, B.; Zheng, H.; Jiang, Y.; Miranda, O. R.; Rotello, V. M.; Xing, B.; Vachet, R. W. Effect of surface charge on the uptake and distribution of gold nanoparticles in four plant species. *Environ. Sci. Technol.* **2012**, *46* (22), 12391–8.
- (22) Michalet, X.; Pinaud, F. F.; Bentolila, L. A.; Tsay, J. M.; Doose, S.; Li, J. J.; Sundaresan, G.; Wu, A. M.; Gambhir, S. S.; Weiss, S. Quantum dots for live cells, in vivo imaging, and diagnostics. *Science* **2005**, *307* (5709), 538–544.
- (23) Whitley, A. R.; Levard, C.; Oostveen, E.; Bertsch, P. M.; Matocha, C. J.; von der Kammer, F.; Unrine, J. M. Behavior of Ag nanoparticles in soil: Effects of particle surface coating, aging and sewage sludge amendment. *Environ. Pollut.* **2013**, *182*, 141–9.
- (24) Whiteside, M. D.; Treseder, K. K.; Atsatt, P. R. The brighter side of soils: quantum dots track organic nitrogen through fungi and plants. *Ecology* **2009**, *90* (1), 100–8.
- (25) Wang, J.; Yang, Y.; Zhu, H.; Braam, J.; Schnoor, J. L.; Alvarez, P. J. Uptake, translocation, and transformation of quantum dots with cationic versus anionic coatings by *Populus deltoides* x *nigra* cuttings. *Environ. Sci. Technol.* **2014**, *48* (12), 6754–62.
- (26) Zhai, G.; Walters, K. S.; Peate, D. W.; Alvarez, P. J.; Schnoor, J. L. Transport of gold nanoparticles through plasmodesmata and precipitation of gold ions in woody poplar. *Env. Sci. Technol. Lett.* **2014**, *1* (2), 146–151.
- (27) Trujillo-Reyes, J.; Vilchis-Nestor, A. R.; Majumdar, S.; Peralta-Videa, J. R.; Gardea-Torresdey, J. L. Citric acid modifies surface properties of commercial CeO₂ nanoparticles reducing their toxicity and cerium uptake in radish (*Raphanus sativus*) seedlings. *J. Hazard Mater.* **2013**, *263* (Pt 2), 677–84.
- (28) Zhao, L.; Hernandez-Viezcas, J. A.; Peralta-Videa, J. R.; Bandyopadhyay, S.; Peng, B.; Munoz, B.; Keller, A. A.; Gardea-Torresdey, J. L. ZnO nanoparticle fate in soil and zinc bioaccumulation in corn plants (*Zea mays*) influenced by alginate. *Environ. Sci. Process Impacts* **2013**, *15* (1), 260–6.
- (29) Lee, S. S.; Song, W.; Cho, M.; Puppala, H. L.; Nguyen, P.; Zhu, H.; Segatori, L.; Colvin, V. L. Antioxidant properties of cerium oxide nanocrystals as a function of nanocrystal diameter and surface coating. *ACS Nano* **2013**, *7* (11), 9693–703.
- (30) Lee, S. S.; Zhu, H. G.; Contreras, E. Q.; Prakash, A.; Puppala, H. L.; Colvin, V. L. High temperature decomposition of cerium precursors to form ceria nanocrystal libraries for biological applications. *Chem. Mater.* **2012**, *24* (3), 424–432.
- (31) Yu, W. W.; Chang, E.; Falkner, J. C.; Zhang, J. Y.; Al-Somali, A. M.; Sayes, C. M.; Johns, J.; Drezek, R.; Colvin, V. L. Forming biocompatible and nonaggregated nanocrystals in water using amphiphilic polymers. *J. Am. Chem. Soc.* **2007**, *129* (10), 2871–2879.
- (32) Zhu, H.; Prakash, A.; Benoit, D. N.; Jones, C. J.; Colvin, V. L. Low temperature synthesis of ZnS and CdZnS shells on CdSe quantum dots. *Nanotechnology* **2010**, *21* (25), 255604.
- (33) Hoagland, D. R.; Arnon, D. I. *The Water-Culture Method for Growing Plants without Soil*; The College of Agriculture: Berkeley, CA, 1950; p 32.
- (34) Wang, J.; Koo, Y.; Alexander, A.; Yang, Y.; Westerhof, S.; Zhang, Q.; Schnoor, J. L.; Colvin, V. L.; Braam, J.; Alvarez, P. J. Phytostimulation of poplars and Arabidopsis exposed to silver nanoparticles and Ag(+) at sublethal concentrations. *Environ. Sci. Technol.* **2013**, *47* (10), 5442–9.
- (35) Goodspeed, D.; Chehab, E. W.; Min-Venditti, A.; Braam, J.; Covington, M. F. Arabidopsis synchronizes jasmonate-mediated defense with insect circadian behavior. *Proc. Natl. Acad. Sci. U.S.A.* **2012**, *109* (12), 4674–7.
- (36) Chehab, E. W.; Kim, S.; Savchenko, T.; Kliebenstein, D.; Dehesh, K.; Braam, J. Intronic T-DNA insertion renders Arabidopsis *opr3* a conditional jasmonic acid-producing mutant. *Plant Physiol.* **2011**, *156* (2), 770–8.
- (37) Meychik, N. R.; Yermakov, I. P. Ion exchange properties of plant root cell walls. *Plant Soil* **2001**, *234* (2), 181–193.
- (38) Terry, N.; Zayed, A. M.; De Souza, M. P.; Tarun, A. S. Selenium in higher plants. *Annu. Rev. Plant Physiol. Plant Mol. Biol.* **2000**, *51*, 401–432.
- (39) Wang, Z.; Xie, X.; Zhao, J.; Liu, X.; Feng, W.; White, J. C.; Xing, B. Xylem- and phloem-based transport of CuO nanoparticles in maize (*Zea mays* L.). *Environ. Sci. Technol.* **2012**, *46* (8), 4434–41.
- (40) Dimkpa, C. O.; McLean, J. E.; Latta, D. E.; Manangon, E.; Britt, D. W.; Johnson, W. P.; Boyanov, M. I.; Anderson, A. J. CuO and ZnO nanoparticles: phytotoxicity, metal speciation, and induction of oxidative stress in sand-grown wheat. *J. Nanopart. Res.* **2012**, *14* (9), 1125–39.
- (41) Servin, A. D.; Morales, M. I.; Castillo-Michel, H.; Hernandez-Viezcas, J. A.; Munoz, B.; Zhao, L. J.; Nunez, J. E.; Peralta-Videa, J. R.; Gardea-Torresdey, J. L. Synchrotron verification of TiO₂ accumulation in cucumber fruit: A possible pathway of TiO₂ nanoparticle transfer from soil into the food chain. *Environ. Sci. Technol.* **2013**, *47* (20), 11592–11598.
- (42) Hernandez-Viezcas, J. A.; Castillo-Michel, H.; Andrews, J. C.; Cotte, M.; Rico, C.; Peralta-Videa, J. R.; Ge, Y.; Priester, J. H.; Holden, P. A.; Gardea-Torresdey, J. L. In situ synchrotron X-ray fluorescence mapping and speciation of CeO₂ and ZnO nanoparticles in soil cultivated soybean (*glycine max*). *ACS Nano* **2013**, *7* (2), 1415–1423.
- (43) Gonzalez-Melendi, P.; Fernandez-Pacheco, R.; Coronado, M. J.; Corredor, E.; Testillano, P. S.; Risueno, M. C.; Marquina, C.; Ibarra, M. R.; Rubiales, D.; Perez-de-Luque, A. Nanoparticles as smart treatment-delivery systems in plants: Assessment of different techniques of microscopy for their visualization in plant tissues. *Ann. Bot.* **2008**, *101* (1), 187–95.
- (44) Giraldo, J. P.; Landry, M. P.; Faltermeier, S. M.; McNicholas, T. P.; Iverson, N. M.; Boghossian, A. A.; Reuel, N. F.; Hilmer, A. J.; Sen, F.; Brew, J. A.; Strano, M. S. Plant nanobionics approach to augment photosynthesis and biochemical sensing. *Nat. Mater.* **2014**, *13* (4), 400–8.